Lysosome Biogenesis Requires Rab9 Function and Receptor Recycling from Endosomes to the *trans*-Golgi Network

Markus A. Riederer, Thierry Soldati, Allan D. Shapiro, Joseph Lin, and Suzanne R. Pfeffer

Department of Biochemistry, Stanford University School of Medicine, Stanford, CA 94305-5307

Abstract. Newly synthesized lysosomal enzymes bind to mannose 6-phosphate receptors (MPRs) in the TGN, and are carried to prelysosomes, where they are released. MPRs then return to the TGN for another round of transport. Rab9 is a ras-like GTPase which facilitates MPR recycling to the TGN in vitro. We show here that a dominant negative form of rab9, rab9 S21N, strongly inhibited MPR recycling in living cells. The block was specific in that the rates of biosynthetic protein transport, fluid phase endocytosis and receptor-mediated endocytosis were unchanged. Expression of rab9 S21N was accompanied by a decrease in the efficiency of lysosomal enzyme sorting. Cells compensated for the presence of the mutant protein by inducing the synthesis of both soluble and membrane-associated lysosomal enzymes, and by internalizing lysosomal enzymes that were secreted by default. These data show that MPRs are limiting in the secretory pathway of cells expressing rab9 S21N and document the importance of MPR recycling and the rab9 GTPase for efficient lysosomal enzyme delivery.

MANNOSE 6-phosphate receptors (MPRs)[1] deliver newly synthesized, soluble lysosomal enzymes from the TGN to pre-lysosomes (Kornfeld and Mellman, 1989; Kornfeld, 1992). Two types of MPRs have been identified to date. One is a 300-kD transmembrane glycoprotein which also binds insulin-like growth factor II; the second is a dimer or tetramer of 45-kD subunits and requires divalent cations for ligand binding in vitro. Both types of MPRs release their ligands upon encountering the low pH within pre-lysosomes, and then return to the Golgi complex to reinitiate another cycle of biosynthetic enzyme transport. MPRs are also present at the cell surface. These receptors are in rapid equilibrium with their intracellular counterparts, and at least the 300-kD MPR is capable of endocytosing extracellular lysosomal hydrolases and delivering them to endocytic compartments.

Work from a number of laboratories has suggested that the rab family of ras-like GTPases plays a key role in regulating receptor trafficking (Zerial and Stenmark, 1993; Pfeffer, 1992). For example, rab5 has been shown to regulate early endosome fusion both in vitro (Gorvel et al., 1991) and in vivo (Bucci et al., 1992). Rab4 functions in receptor recycling between early endosomes and the cell surface (van der Sluijs et al., 1992). In addition, rab1 and its yeast homolog, YPT1, play a key role in the transport of proteins between the ER and the Golgi (Plutner et al., 1991; Tisdale et al., 1992; Rexach and Schekman, 1991; Segev, 1991). Rab proteins are thought to function in transport vesicle targeting and/or fusion events, because *SEC4* mutant yeast strains accumulate secretory vesicles (Novick et al., 1980), anti-*YPT1* antibodies inhibit ER-derived transport vesicle fusion (Rexach and Schekman, 1991; Segev, 1991; Plutner et al., 1991), and anti-rab5 antibodies block early endosome fusion (Gorvel et al., 1991).

We showed recently that the rab9 protein is localized primarily to the surface of late endosomes and can facilitate the transport of MPRs from late endosomes to the TGN in vitro (Lombardi et al., 1993). To investigate the physiological significance of our findings, and to explore the significance of MPR recycling in living cells, we generated a dominant inhibitory form of rab9 protein based upon well characterized mutations of Ras. In this report, we demonstrate that rab9 protein is required for MPR recycling between late endosomes and the TGN in vivo. In addition, we describe the physiological consequences of blocking this transport pathway. Our experiments confirm the importance of the MPR in TGN sorting of lysosomal hydrolases. Moreover, they highlight several types of compensatory mechanisms by which cells can bypass the biosynthetic transport pathway for lysosomal enzymes.

Materials and Methods

Rabbit anti-bovine MPR antiserum (Pfeffer, 1987), rabbit and mouse anti-rab9 antibodies (Soldati et al., 1993*a*), and anti-lgpB antibodies (Miettinen et al., 1989) were previously characterized reagents. β-glucuronidase, rabbit anti-cathepsin D, mouse anti-CHO lgpB, and rabbit anti-TGN38 were the generous gifts of Drs. Stuart Kornfeld (Washington University, St. Louis, MO), William Sly (St. Louis University, St. Louis,

Address all correspondence to S. Pfeffer, Department of Biochemistry, B400, Stanford University Medical School, Stanford, CA 94305-5307.

1. *Abbreviations used in this paper*: ECL, enhanced chemiluminescence; man6P, mannose 6-phosphate; MPR, mannose 6-phosphate receptor.

MO), Ira Mellman (Yale University, New Haven, CT), and George Banting (University of Bristol, Bristol, U.K.), respectively. Unless otherwise indicated, reagents were from Sigma Chemical Company (St. Louis, MO). Protein was determined by BCA assay (Pierce Chemical Co., Piscataway, NJ) or Bradford assay (Bradford, 1974) using bovine serum albumin as standard.

Rab9 Mutagenesis and Expression

To facilitate subcloning of the rab9 cDNA, a PvuII site was introduced downstream of the stop codon using the oligonucleotide $^{5'}$GGCAGCTGTCAACAGCAAGATGAGCT$^{3'}$. The plasmid pET8c-rab9 (Lombardi et al., 1993) served as template for the PCR reaction. A rab9-containing fragment was obtained using the T7 sequencing primer hybridizing to the T7 promoter of the plasmid and the PvuII containing primer which hybridized downstream of the stop codon. Mutagenesis was confirmed by sequencing. The oligonucleotide, $^{5'}$GGGAAGAACTCTCTAATG$^{3'}$ was used to obtain the rab9S21N mutant using PCR in combination with the same primers used to introduce the PvuII site. Wild type and mutant rab9 cDNAs were cloned into the mammalian expression vector, pCVN, under the control of the SV40 early promoter, or into the *Escherichia coli* expression vector, pET8c (Studier et al., 1990), under the control of the T7 promoter. To generate the plasmids, pCVN-4rab9wt, pCVN-rab9S21N, and pET8c-rab9S21N, the PCR products were digested with NcoI and PvuII, the vector pET8c was digested with NcoI and BamHI, and pCVN was digested with ClaI. DNA fragments were purified by agarose gel electrophoresis. For the mammalian vectors, the NcoI sticky end of the rab9 and rab9 S21N fragments, and the ClaI sticky ends of the vector pCVN were filled with the Klenow fragment of DNA polymerase I. The BamHI site of pET8c was filled with Klenow. DNA fragments were purified using the gene clean procedure (Bio 101 Inc., Vista, CA) prior to ligation (Maniatis et al., 1989), which was confirmed by restriction analysis. BL21 (DE3) (F^-, ompT, r^-_B, m^-_B) (Studier et al., 1990) was transformed with pET8c-rab9S21N for *E. coli* expression of rab9 S21N.

Purification of rab9 S21N

Purification of rab9 S21N was by a modification of our previous method (Shapiro et al., 1993). IPTG induction was for 6 h at 30°C. Centrifugation was for 1.5 min, using a setting of 20,000 rpm in a rotor (JA-20; Beckman Instruments, Palo Alto, CA). Protamine sulfate was added to 2 mg/ml, and the suspension was stirred for 1 min. The supernatant was loaded onto a 15 ml Q-Sepharose column using a peristaltic pump. Sephacryl S-100 fractions containing rab9 S21N were pooled and diluted 1:1 with buffer A (64.4 mM Tris-HCl, pH 8.0, 8 mM $MgCl_2$, 2 mM EDTA, 0.5 mM DTT, 10 μM GDP, 10 mM benzamidine). The sample was then filtered through a 0.2-μm filter (Gelman Science, Inc., Ann Arbor, MI) and applied to a 1 ml FPLC Mono Q column pre-equilibrated with buffer A. The column was washed with 24 ml of buffer A and subsequently eluted with a 15 ml gradient of 0–200 mM NaCl in buffer A. Fractions of 0.5 ml (30) were collected; those containing full-length rab9 S21N (≥90% pure) were pooled and concentrated.

Biochemical Characterization of rab9 S21N

Relative affinities of wild type and S21N rab9 for GDP vs. GTP were determined by incubating 200 nM wild type rab9 or 180 nM rab9 S21N with 3 μM [8,5'-^{3}H]GDP (Du Pont-New England Nuclear, Boston, MA) and the specified level of unlabeled GTP at 32°C in 50 mM Hepes-KOH (pH 7.4), 150 mM KCl, 5 mM $MgCl_2$, 4.5 mM EDTA, 1 mM DTT, 0.1% BSA. After either 15 min or 2 h the reactions were stopped and nucleotide binding was assayed by filtration (Shapiro et al., 1993). Rates of nucleotide exchange were measured as rates of binding of [8,5'-^{3}H]GDP for rab9 S21N (which was purified as a 1:1 complex with unlabeled GDP) (Shapiro et al., 1993); incubations were brought to 37°C prior to addition of rab9 S21N or nucleotide. Rab9 S21N was then added to 180 nM, the mixture was vortexed for 5 s, and nucleotide was added to 3 μM. Tubes were vortexed, returned to 37°C, and time points were taken as described. Both rab9 and rab9 S21N bound nucleotide in a saturable and stable fashion for at least 15 min under all conditions assayed. Free Mg^{2+} concentrations were calculated by published methods (Sunyer et al., 1984).

Cell Lines

CHO wild type cells or the CHO ldlD cell line (Kingsley et al., 1986; purchased from American Type Culture Collection, Rockville, MD) were transformed with pCVN, pCVNrab9 or pCVNrab9S21N by electroporation. Stable transformants were selected by resistance to neomycin (Geneticin, G418; GIBCO BRL, Gaithersburg, MD; 400 μg/ml) and single clones were isolated and confirmed for rab9 expression by indirect immunofluorescence. The expression level of rab9 was quantified by Western blot (Burnette, 1981) using rabbit anti-rab9 and HRP conjugated goat anti-rabbit antibodies at a 1:1000 dilution. Rab9 was detected by enhanced chemiluminescence (ECL; Amersham Corp., Arlington Heights, IL) followed by densitometer scanning.

Determination of Surface Localized MPR

Cells were grown to subconfluency and labeled overnight at 37°C with [^{35}S]methionine and cysteine (Translabel, Amersham Corp.; 100 μCi/ml) in αMEM lacking cysteine and methionine but containing 10% dialyzed fetal calf serum. Cells were chilled on ice and washed twice with ice cold TD (25 mM Tris-HCl, pH 7.4, 5.4 mM KCl, 137 mM NaCl, 0.3 mM Na_2HPO_4) and once with ice cold TD + 0.1% BSA. Rabbit anti-MPR antiserum (6 μl) was allowed to bind to surface-localized MPRs for 3 h at 4°C. Excess unbound antibodies were removed by three washes with TD, 0.1% BSA and the cells were solubilized with 0.4 ml RIPA (20 mM Na phosphate, pH 7.5, 0.15 M NaCl, 1% Triton X-100, 0.5% deoxycholate, and 0.1% SDS). After centrifugation at 100,000 *g* for 10 min at 4°C, the supernatant was transferred to a new tube; immune complexes were harvested by addition of 100 μl of *Staphylococcus aureus* cells (Pansorbin, Calbiochem) for 1 h at 4°C, followed by centrifugation. The supernatant containing intracellular MPRs was incubated with 6 μl of anti-MPR antiserum for 1 h, and immune complexes were harvested as before. Both pellets were washed 3× with RIPA, 1× with RIPA + 500 mM NaCl, and 1× with TD before they were resuspended in 45-μl sample buffer and boiled for 5 min. Proteins were resolved by 8% SDS-PAGE (Laemmli, 1970) and quantified with a Phosphorimager (Molecular Dynamics Inc., Sunnyvale, CA).

Determination of Membrane-associated rab9

Cells were swollen and scraped as previously described (Goda and Pfeffer, 1988). Membranes and cytosol were separated using a sucrose gradient centrifugation step (Soldati et al., 1993*a*). Samples of membrane and cytosol fractions were resolved by 12.5% SDS-PAGE and rab9 was detected by Western blotting and ECL.

MPR Recycling from the Cell Surface to the TGN

The assay was essentially as described by Duncan and Kornfeld (1988). Cells were grown in 6-cm dishes in αMEM, 10% FCS to ~60% confluency and labeled with [^{35}S]methionine and cysteine (100 μCi/ml) overnight at 37°C. After a 2 h chase in complete media (αMEM, 10% FCS), cells were washed once in TD and once in αMEM, 1% FCS. Sialic acid residues on surface localized MPRs were removed enzymatically by the addition of 0.02 U *Vibrio cholerae* neuraminidase in 1 ml αMEM, 1% FCS, 20 mM Hepes, pH 7.4. After 2 h at 37°C the cells were washed four times with TD and twice with αMEM, 10% FCS, before they were recultured at 37°C in αMEM, 10% FCS. Transport was stopped by chilling the cells on ice; MPRs were solubilized in 0.4 ml detergent stop mix (Goda and Pfeffer, 1988) and centrifuged at 100,000 *g* for 10 min at 2°C. The supernatant was transferred to a new tube and the fraction of sialic acid–containing MPRs was determined by slug lectin chromatography (Goda and Pfeffer, 1988). Proteins were separated by 8% SDS-PAGE and quantification was performed with a Phosphorimager (Molecular Dynamics).

Endocytosis of HRP and β-Glucuronidase

HRP uptake was measured as previously described (Bucci et al., 1992) using cells grown to 50% confluency in 6 cm dishes. Endocytosed HRP activity was assayed using *o*-dianisidine as substrate (Marsh et al., 1987). To measure uptake of β-glucuronidase, cells were grown to subconfluency in 35 mm dishes and washed twice with PBS. Binding buffer (αMEM, 10 mg/ml BSA) containing 10 nM β-glucuronidase was added to each dish and incubated at 37°C for various times. Dishes were transferred onto an ice-cold metal block and incubated for 1 h at 4°C to allow complete surface binding of β-glucuronidase. Supernatants were aspirated and cells were washed 5× with PBS + 10 mg/ml BSA. Surface bound β-glucuronidase was stripped from the cell surface by two washes with 0.5 ml, 50 mM citrate-phosphate, pH 5.0, 150 mM NaCl and transferred into a separate tube. Intracellular β-glucuronidase was recovered by solubilizing cells in 0.5

ml, 10 mM Tris-Cl pH 7.4, 0.1% Triton X-100, 150 mM NaCl. β-glucuronidase activity was assayed (Robbins, 1979) using 4-methylumbelliferyl-glucuronide as a substrate. 1 U was defined as the amount of enzyme needed to yield 1 nmol product in 1 h at 37°C.

Hexosaminidase Secretion

The assay was modified from that described by Robbins (1979). Cells were grown in complete medium to subconfluency in 6 cm dishes. The medium was removed and the cells washed 2× with TD before 1 ml of prewarmed OPTI-MEM (GIBCO BRL; with or without 10 mM mannose 6-phosphate) was added to each dish. After 6 or 8 h at 37°C, secreted hexosaminidase activity was assayed in 0.5 ml media by addition of 120 μl 5× hexosaminidase substrate buffer (0.5 M NaAcetate, pH 4.4, 0.5% Triton X-100, 5 mM *p*-nitrophenyl-*N*-acetyl-β-D-glucosaminide). After 1 h at 37°C, reactions were stopped by addition of 0.6 ml of 0.5 M glycine, 0.5 M Na_2CO_3, pH 10.0. Release of *p*-nitrophenol was measured spectrophotometrically at 405 nm. 1 U of enzyme activity was defined as the amount of enzyme needed to hydrolyze 1 nmol per hour at 37°C. Intracellular hexosaminidase was determined by scraping the cells in 10 mM phosphate buffer, pH 6.0, 0.15 M NaCl, 0.5% Triton X-100 followed by centrifugation at 100,000 *g* for 10 min at 2°C. The supernatant was transferred into a fresh tube and a portion was assayed for hexosaminidase activity. Generally, 25 μl of cell extract was mixed with 500 μl of 1× hexosaminidase substrate buffer.

Cathepsin D Maturation

Cells were grown to subconfluency and pulse labeled for 30 min as described above. Cells were then washed 3× with TD and chased in αMEM, 10% FCS for up to 4 h. At various time points, cells were placed on ice, washed 2× with ice cold TD, and then solubilized in 0.4 ml RIPA. After centrifugation at 100,000 *g*, the supernatant was transferred into a new tube and immunoprecipitated with rabbit anti-cathepsin D antibodies at a dilution of 1:200. It is important to note that the antibody displayed highest affinity to mature cathepsin, and could not be used to monitor the secretion of the precursor.

Immunofluorescence Microscopy

Immunofluorescence was performed as described by Warren et al. (1984) using cells grown on collagen-coated glass coverslips. Texas red- or FITC-conjugated second antibodies were used at a dilution of 1:500. Slides were viewed using a 100× objective on a Zeiss Axiophot microscope.

Results

We used site-directed mutagenesis to generate rab9 mutant proteins which might block intracellular transport upon expression in mammalian cells. The most informative mutant was rab9 S21N. This mutation is equivalent to Ras S17N, a dominant inhibitory mutation of the Ras protein (Feig and Cooper, 1988; Farnsworth and Feig, 1991). In Ras, serine 17 has been postulated to participate through its hydroxyl moiety in the coordination of a magnesium ion at the active site (Pai et al., 1989, 1990). Ras S17N binds GDP in strong preference over GTP, and appears to act as a dominant inhibitor by sequestering a nucleotide exchange factor, thus increasing the concentration of Ras-GDP (Feig and Cooper, 1988). This hypothesis was confirmed directly for an analogous mutation in rab3A (T36N) which was shown to bind with 10-fold greater affinity than wild type rab3A to a rab3A-specific, nucleotide exchange factor (Burstein et al., 1992).

We measured the relative affinities of wild type rab9 and rab9 S21N for GDP versus GTP to determine if the mutant rab9 protein resembled ras S17N in terms of its nucleotide binding characteristics. As shown in Fig. 1 *A*, wild type rab9 (*open circles*) displayed identical affinities for GDP and GTP: when presented with an equimolar ratio of GTP and ^{3}H-GDP, approximately 50% of the molecules bound GDP. However, rab9 S21N (*filled circles*) showed an approximately 50-fold greater preference for GDP. Thus, analogous to RasS17N, rab9 S21N displayed preferential binding of GDP relative to GTP. While the GDP off-rate from wild type Ras protein shows a strong dependence upon magnesium ion concentration, the GDP off-rate for Ras S17A appears to be independent of magnesium (John et al., 1993). A similar lack of dependence upon magnesium concentration was also detected for the off-rate of GDP from rab9 S21N (Fig. 1 *B*). Together, these data confirm that rab9 S21N displays the expected in vitro properties for a dominant inhibitory mutant of a ras-like GTPase.

Expression of rab9 S21N In Vivo

A stable CHO cell line expressing rab9 S21N (N21) was generated by conventional means. As shown in Fig. 2, these cells expressed a protein of ~25 kD that was recognized by monoclonal anti-rab9 antibodies upon immunoblot analysis. Quantitation of immunoblots indicated that the rab9 S21N protein was expressed at approximately twofold higher levels than the endogenous, wild type rab9 protein. N21 cells displayed the same doubling time as wild type cells, and showed no obvious morphological changes, except that they displayed contact inhibition at a lower cell density.

Total N21 cell extracts contained two anti-rab9 antibody immunoreactive polypeptides (Fig. 2, *total*). The upper band is likely to represent non-prenylated rab9 S21N since its mobility was similar to rab9 protein expressed in *E. coli* and it was primarily cytosolic. In addition, gel filtration analysis indicated that unlike the wild type protein (Soldati et al., 1993), rab9 S21N was present in the cytosol as a monomer, not associated with GDI, a protein which solubilizes cytosolic, prenylated rab proteins. The lower band in Fig. 2 (*N21*, total) is likely prenylated, since it was only present in membrane fractions and electrophoresed with a mobility similar to prenylated, wild type rab9. We have shown elsewhere that prenylated rab9 electrophoreses faster than non-prenylated rab9 (Soldati et al., 1993).

While 80–90% of overexpressed wild type rab9 was membrane associated in control cells, only ~20–25% of the rab9 S21N was membrane-associated in N21 cells. The extent of membrane association appeared to match the fraction of rab9S21N that was geranylgeranylated (Fig. 1). These data suggest that rab9 S21N is a poorer substrate for rab prenyltransferase than wild type rab9. This conclusion was confirmed using an in vitro prenylation assay and purified rab9 and rab9 S21N proteins, according to our published procedure (Soldati et al., 1993; and data not shown).

Rab9 S21N Blocks Endosome-to-TGN Transport In Vivo

We have shown that rab9, but not rab4 or rab7, can stimulate the transport of MPRs from late endosomes to the TGN in vitro (Lombardi et al., 1993). To explore the effect of rab9 S21N on this pathway in vivo, we used an assay devised by Kornfeld and colleagues to detect the transport of proteins from the cell surface to the TGN in living cells (Duncan and Kornfeld, 1988). Metabolically labeled surface MPRs were desialylated by incubation of cells with neuraminidase at 37°C. Under these conditions, a large proportion of MPRs cycle through the surface, where they can be acted upon by

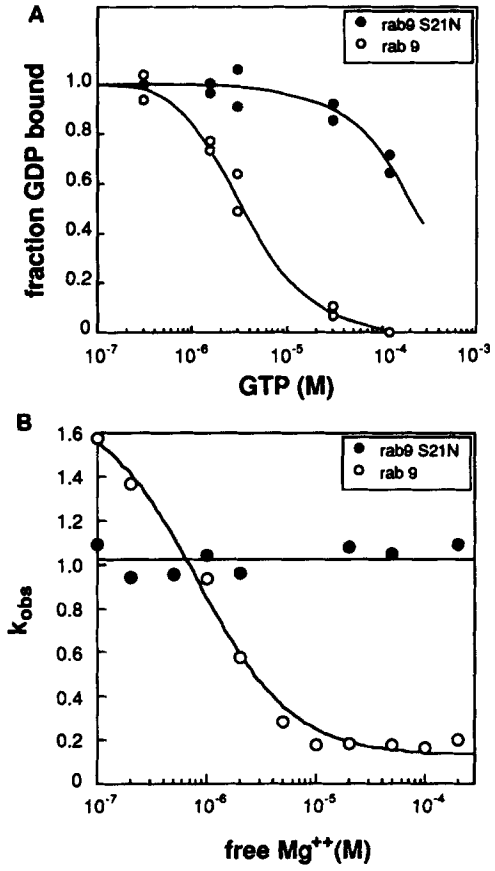

Figure 1. Rab9 S21N interacts with nucleotides in vitro in the predicted fashion. (*A*) 200 nM rab9 (○) or 180 nM rab9 S21N (●) was incubated with 3 μM [8,5'-^{3}H]GDP and varying levels of unlabeled GTP at 32°C for 2 h. Reactions were stopped and assayed for protein-bound nucleotide as described in Materials and Methods. Identical results were obtained if reactions were stopped after only 15 min. (*B*) Nucleotide exchange for rab9 (○) or rab9 S21N (●) was assessed over time points up to 15 min, and the data were fitted to first-order exponential functions using Kaleidagraph software. The observed rate constants for nucleotide exchange were plotted versus the free magnesium ion concentration used for each experiment; the data for wild type rab9 were fitted to the equation described below. The dissociation of nucleotide from ras has been shown to behave according to the following equation:

$$k_{obs} = \frac{k_{-3}}{1 + K_D/[Mg^{2+}]} + \frac{k_{-2}}{1 + [Mg^{2+}]/K_D}$$

where k_{obs} = the observed nucleotide exchange rate constant, K_D = the equilibrium dissociation constant describing the affinity of magnesium ion for the ras·GDP complex, $[Mg^{2+}]$ = the concentration of free magnesium ion, k_{-3} = the first order rate constant for dissociation of GDP·Mg^{2+} from ras·GDP·Mg^{2+}, and k_{-2} = the first order rate constant for dissociation GDP from ras·GDP (John et al., 1993). This model assumes that bound magnesium is in rapid equilibrium with the solvent. This was tested for wild type ras and for rab9 (not shown) by showing that the nucleotide exchange rate switches from a rate characteristic of high free magnesium to one of low free magnesium immediately upon addition of EDTA. Because dissociation of bound magnesium is fast on the time scale of nucleotide exchange (implying $k_{-2} >> k_{-3}$) the form of a curve fit to this equation will be dominated by the second term. Data from wild type rab9 generated a curve which displays an approximately hyperbolic decrease when $k_{-3} < k_{obs} < k_{-2}$. Fitted constants were 1.7 min^{-1} for k_{-2}, 0.13 min^{-1} for k_{-3}, and 820 nM for K_d as compared with 0.22 min^{-1}, 9.7 × 10^{-4} min^{-4} min^{-1}, and 2.8 μM for ras, respectively (John et al., 1993). Comparing rab9 with ras, magnesium ion binding to the protein·nucleotide complex is of slightly higher affinity and dissociation of both magnesium ion and magnesium·GDP from the ternary complex are faster for rab9; however, like ras, rab9 appears to behave according to the equation above. For rab9 S21N, k_{obs} is approximately equal to 1 min^{-1} and is independent of free magnesium concentration. Identical results were obtained for ras S17A (John et al., 1993), implying in both cases that k_{-2} is approximately equal to k_{-3}.

the neuraminidase. Cells are then washed and incubated further to permit endocytosis and intracellular transport. Unlike most receptors which remain in the endocytic pathway, MPRs return to the TGN and can be modified by the sialyltransferases located there. The re-acquisition of sialic acid by MPRs over time can then be determined by chromatography on a column of a sialic acid–specific lectin (Goda and Pfeffer, 1988).

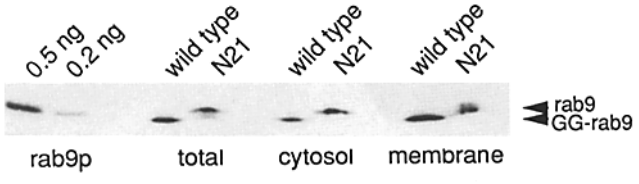

Figure 2. N21 cells express rab9 S21N protein. Cells expressing wild type rab9 (*wild type*) or rab9 SN21 (*N21*) were fractionated into membrane and cytosol fractions and analyzed for the presence of rab9p by immunoblot analysis. Lanes *1* and *2*, rab9 protein purified from an *E.* coli expressing strain; lanes *3* and *4*, total extracts; lanes *5* and *6*, cytosol fractions; lanes *7* and *8*, membrane fractions. For this experiment, clone 2 cells were analyzed which express wild type rab9 at ~50-fold higher levels than control cells; sample volumes were adjusted to yield ~0.5 ng rab9 in each gel lane. The arrows at right indicate the electrophoretic mobilities of unprenylated rab9 (*rab9*) and prenylated rab9 (*GG-rab9*).

As shown in Fig. 3, in control cells, a significant fraction of MPRs re-acquired sialic acid during a 3-h postneuraminidase incubation, at a rate comparable to previous reports (Duncan and Kornfeld, 1988; Chege and Pfeffer, 1990). In contrast, MPR resialylation was inhibited dramatically in cells expressing rab9 S21N. Resialylation was not completely blocked, but displayed a lag of ≥3 h. Thus, rab9 S21N displayed a dominant phenotype when expressed at twofold higher levels than endogenous rab9, and interfered with the process by which MPRs are recycled to the TGN in living cells.

It is not yet known whether cytosolic or membrane associated rab9 S21N was responsible for the inhibition observed. However, it is interesting to note that if only the membrane-associated S21N protein was inhibitory, it would have been present on the membrane at roughly 40% the level of endogenous rab9 protein. It seems most likely that the delayed resialylation of MPRs seen in N21 cells reflects a significant but incomplete block of MPR recycling, as would be expected, given a mutant protein that is predicted to interfere with rab9–nucleotide exchange factor interactions.

Rab9 S21N Inhibition Is Specific to Endosome–TGN Transport

According to current models of rab function, a mutant rab protein should display a defect along a single route of intra-

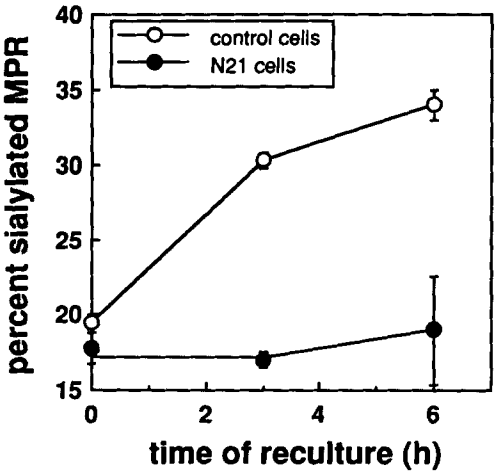

Figure 3. Rab9 S21N blocks MPR recycling to the TGN in vivo. Control cells (○) and N21 cells (●) were metabolically labeled, treated with neuraminidase, and then recultured for the times indicated. The reappearance of sialic acid–containing MPRs was then determined as described in Materials and Methods. Values shown represent the average of duplicate measurements derived from two experiments carried out in duplicate; percent sialylated MPR is expressed relative to the amount of total cellular MPRs, ±SEM.

cellular transport. To verify the specificity of rab9 action, we investigated the capacity of cells expressing rab9 S21N to carry out both fluid phase and receptor-mediated endocytosis. As shown in Fig. 4, wild type cells and N21 cells displayed identical rates of horseradish peroxidase uptake. Thus, fluid phase endocytosis was unaltered by rab9 S21N overexpression.

Receptor-mediated endocytosis was tested by monitoring the ability of N21 cells to bind and internalize extracellularly administered β-glucuronidase via cell surface MPRs. At time zero, N21 cells were found to contain almost twofold more endogenous β-glucuronidase than control cells (Fig. 5; Table I). As will be described below, N21 cells also contained higher levels of several other lysosomal enzymes. In addition, N21 cells possessed 3.9 times as many surface

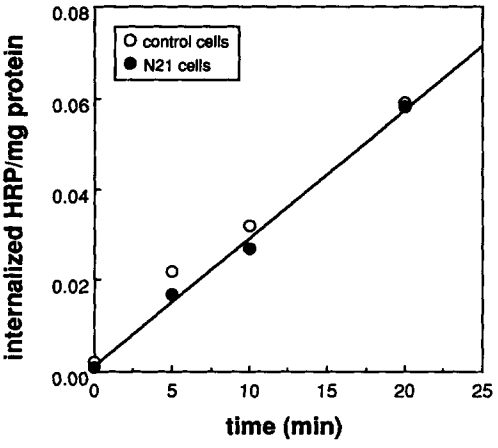

Figure 4. Rab9 S21N expression does not affect fluid phase endocytosis. Control cells (○) or N21 cells (●) were incubated with HRP and internalized HRP was monitored as described in Materials and Methods. Values shown represent the average of triplicate determinations from a representative experiment.

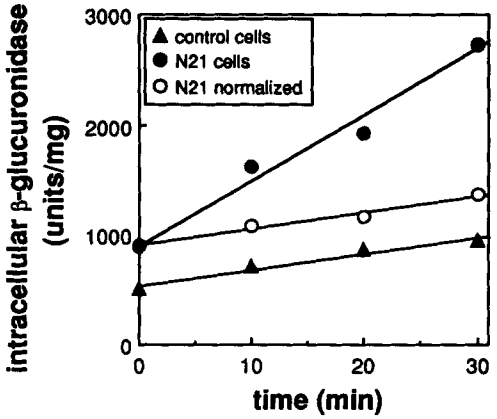

Figure 5. Rab9 S21N does not alter the rate of MPR-mediated endocytosis. Cells were incubated with β-glucuronidase for various times. Surface bound and intracellular β-glucuronidase activity were assayed as described in Materials and Methods; values are the average of duplicates from a representative experiment. Control cells (▲), N21 cells (●), and N21 cells normalized for surface β-glucuronidase binding site differences (○; to obtain an endocytosis rate per surface binding site, N21 values were divided by 3.9).

binding sites for β-glucuronidase than the control cells, which correlated with an increase in the level of MPRs in these cells (see below).

N21 cells internalized more total β-glucuronidase per unit time than the control cells. However, when the rate of β-glucuronidase uptake in N21 cells was corrected for the difference in surface binding sites (Fig. 5, *N21 normalized*), the absolute rates of enzyme internalization per surface binding site were identical for N21 and control cells. These data confirm that the pathway of receptor-mediated endocytosis is not influenced by rab9 S21N protein expression. Moreover, they show that the 300-kD MPRs are functional in N21 cells in terms of their capacity for ligand binding and receptor-mediated endocytosis.

The specificity of the transport block induced by rab9 S21N expression was confirmed by examining the rate of biosynthetic protein transport of glycoproteins through the secretory pathway. For this purpose, we examined the rate with which the 300-kD MPR was transported from the endoplasmic reticulum to the medial Golgi apparatus, as monitored by the rate with which it acquired endoglycosidase H–resistant oligosaccharides. As expected, rab9 S21N had no influence on the rate of biosynthetic protein transport; MPRs in control and N21 cells acquired endoglycosidase H–resistant oligosaccharides with a half-time of ~60 min in CHO cells, consistent with previous reports (Sahagian and Neufeld, 1983).

Rab9 S21N Interferes with Lysosomal Enzyme Targeting

The recycling of MPRs from late endosomes to the TGN is believed to be an important step in the delivery of newly synthesized lysosomal enzymes from the TGN to prelysosomes. If rab9 S21N blocks this process selectively, expression of rab9 S21N should decrease the number of available MPRs within the TGN, and thus interfere with the targeting of newly synthesized lysosomal hydrolases. To test this possibility, we investigated the rate of appearance of newly syn-

Table I. Rab9 S21N Induces Compensatory Lysosome Biogenesis

	Cellular content		
	Control cells	N21 cells	Four independent S21N clones*
300-kD MPR (total)	1.0	1.6 ± 0.2 (3)	1.5 ± 0.06
300-kD MPR (surface)	7.5% ± 1.0% (3)	11.7% ± 1.6% (3)	
cathepsin D	1.0	1.6 ± 0.24 (3)	
hexosaminidase	1,132 u/mg	1,843 u/mg	
(relative level)	1.0	1.63 ± 0.11 (4)	1.42 ± 0.11
β-glucuronidase	476 u/mg	912 u/mg	
(relative level)	1.0	2.2 ± 0.3 (2)	
lgpB (relative level)	1.0	3.6 ± 0.3 (4)	3.25 ± 0.81

Enzyme assays of cellular content were as described in Materials and Methods. The lysosomal glycoprotein lgpB was monitored by immunoblot using monoclonal anti-lgpB antibodies, ^{125}I-labeled protein A, followed by Phosphorimager quantification. MPR and cathepsin D expression levels were determined by immunoprecipitation of ^{35}S-labeled proteins followed by SDS-PAGE and Phosphorimager quantification. Values presented are averages ± standard error of the mean; the number of measurements used is shown in parentheses.

* These clones expressed rab9 S21N at an average of 2.23 (±0.28)-fold higher levels than endogenous rab9 wild type protein.

thesized cathepsin D into late endosomes and/or lysosomes. Cathepsin D is synthesized as a 50-kD precursor, which is slowly converted to a 31-kD mature form upon arrival in prelysosomes and/or lysosomes (Rosenfeld et al., 1982; Erickson and Blobel, 1983). This processing event thus provided a convenient means to monitor lysosomal enzyme targeting.

Fig. 6 shows the rate with which the 31-kD mature form of cathepsin D was generated in control and N21 cells. As expected, the expression of rab9 S21N had severe consequences in terms of the delivery of cathepsin to prelysosomes and/or lysosomes. The rate with which cathepsin D was processed, indicative of MPR-dependent targeting, was more than threefold lower in N21 cells when compared with control cells.

These results are due either to a decrease in the rate of delivery of newly synthesized cathepsin D to lysosomes, or to a decrease in the levels of processing enzymes that are present in late endosomes and/or lysosomes. According to either of these scenarios, the data support a model in which MPR recycling to the TGN is required for efficient lysosomal enzyme targeting, and suggest further that MPRs are limiting components in the lysosomal targeting pathway.

If the receptor-mediated delivery of newly synthesized lysosomal enzymes from the TGN to lysosomes is disrupted, cells expressing rab9 S21N should display an increased level of lysosomal enzyme secretion via a bulk-flow, default pathway. This prediction was confirmed upon analysis of the secretion of newly synthesized hexosaminidase from control and N21 cell lines (Fig. 7). Control cells and N21 cells synthesized hexosaminidase at identical rates (~14 U/mg/h). However, N21 cells secreted more than twice as much of the newly synthesized hexosaminidase as control cells. Assays of enzyme secretion were carried out in the presence of excess mannose 6-phosphate (*man6P*) to block interaction with surface MPRs. Omission of man6P led to a decreased ac-

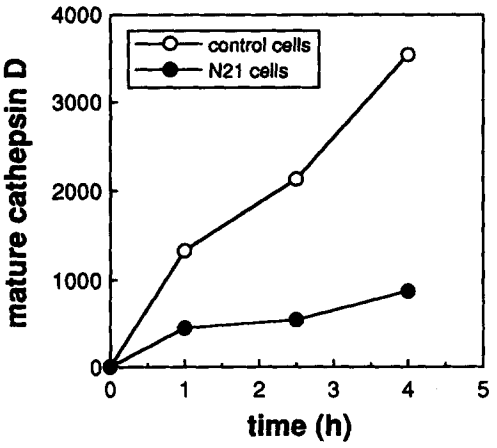

Figure 6. Rab9 S21N inhibits delivery of cathepsin D to lysosomes. Control cells (○) and N21 cells (●) were grown to subconfluency, metabolically labeled for 0.5 h, and then chased for up to 4 h at 37°C. The appearance of mature, 31-kD cathepsin D was monitored at each chase time point by immunoprecipitation, SDS-PAGE, and Phosphorimager quantitation. The average of duplicate determinations from a representative experiment is shown. N21 cell values were divided by 1.5 to obtain a rate of transport per molecule synthesized.

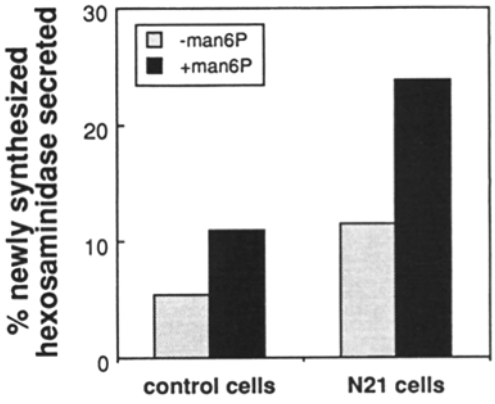

Figure 7. Rab9 S21N increases secretion of hexosaminidase. Subconfluent cells were washed and secretion of newly synthesized hexosaminidase into freshly added medium was measured after 6-h incubation in the presence (*black bar*) or absence (*gray bar*) of 10 mM mannose 6-phosphate. Hexosaminidase activity was assayed as described in Materials and Methods and normalized to protein concentration of harvested cells. Newly synthesized hexosaminidase was defined as the increase of intracellular plus extracellular hexosaminidase activity in 6 h. Values shown represent the average of duplicate determinations from a representative experiment.

cumulation of hexosaminidase in the extracellular medium, indicating that the cells were able to re-internalize the secreted enzyme. The ability of man6P to increase the levels of detected secreted hydrolases confirmed that MPRs were fully functional in terms of their capacity to endocytose extracellular lysosomal hydrolases. In summary, N21 cells secreted a larger proportion of their lysosomal enzyme content than control cells, and compensated for this by an endocytic recapture process.

Rab9 S21N Induces Compensatory Lysosome Biogenesis

As summarized in Table I, N21 cells contained 1.6-fold more hexosaminidase and 2.2-fold more total β-glucuronidase. They also contained higher levels of cathepsin D. Cells could have acquired higher steady state levels of lysosomal enzymes by an increased rate of synthesis, increased endocytic recapture, or a decrease in lysosomal enzyme turnover. Although the rate of hexosaminidase synthesis was identical in N21 and control cells, increased synthesis was detected for cathepsin D; N21 cells synthesized ~1.5× as much of this protein during a 30-min pulse-labeling period as control cells. Surprisingly, the cells also contained higher levels of a lysosomal membrane glycoprotein which does not utilize MPRs for delivery to lysosomes. N21 cells contained 3.6 times as much lgpB as control CHO cells (Table I). In addition, N21 cells had increased levels of MPRs. This increase in MPR number was not due to a constant rate of synthesis accompanied by a slower rate of protein turnover, since the half-life of MPRs actually decreased slightly from 13 h to 10 h in N21 cells. This suggests that a large portion of the pathway of lysosome biogenesis was amplified in the N21 cell line.

To ensure that the increase in lysosomal proteins and MPRs was not an unusual feature of the N21 clonal cell line, we also examined the levels of hexosaminidase, lgpB and the 300-kD MPR in four independently isolated cell clones expressing rab9 S21N at amounts comparable to the N21 cells (~twofold higher than endogenous rab9). As summarized in Table I, the four cell lines all displayed a phenotype very similar to N21, expressing higher levels of MPRs, hexosaminidase and lgpB. Further overexpression of rab9 S21N protein to as high as twenty fold over the level of the endogenous wild type rab9 protein did not yield a further increase in lysosomal enzyme levels (not shown).

MPR Localization Is Not Dramatically Altered in N21 Cells

The experiments presented above suggested that in N21 cells, MPR trafficking through the secretory and endocytic pathways was unaltered, and that the only step blocked by rab9 S21N expression was recycling from late endosomes to the TGN. Under these conditions, one would expect that the steady state distribution of MPRs would be unchanged. Indirect immunofluorescence of N21 cells confirmed this conclusion. As shown in Fig. 7, the overall morphological distribution of MPRs appeared to be very similar in N21 and control cells (Fig. 7, *top row*). The bulk of the receptors were present in perinuclear organelles that are likely to represent late endosomes and to a smaller extent, the TGN (Geuze et al., 1984, 1985, 1988; Griffiths et al., 1988, 1990).

N21 cells expressed 1.6-fold more 300-kD MPRs than control cells, and a larger fraction of their total MPRs were present at the cell surface at steady state (Table I). Taken together, this would lead to an approximately 2.5-fold increase in the absolute number of surface 300-kD MPRs on N21 cells. As would be expected, the block in transport between late endosomes and the TGN seemed to increase the pool of receptors transiting along the endocytic pathway. Nevertheless, at steady state, the vast majority were still present in intracellular compartments.

The fact that the general distribution of MPRs did not change in N21 cells suggests that a block in recycling to the TGN does not influence the rates of other MPR intracellular transport events. These results also imply that exit from late endosomes is rate-limiting for overall MPR transport.

The morphology of lgpB-positive structures (lysosomes and late endosomes) seemed normal in N21 cells (Fig. 8). The increased cellular content of lgpB appeared to be matched by an increase in the apparent number of lysosomes and an increase in perinuclear staining in N21 cells. In addition, the TGN, as monitored by the distribution of TGN38, did not appear to be altered, at least at the level of immunofluorescence microscopy. Finally, the fraction of rab9 S21N that was membrane-associated displayed a distribution that resembled that of MPRs and wild type rab9 protein (Lombardi et al., 1993). The apparently normal morphology of late endosomes, lysosomes, and the TGN in N21 cells supports the contention that the cells are not generally poisoned by low level expression of rab9 S21N.

Discussion

We have shown here that the Ras-like GTPase, rab9, is essential for the recycling of 300-kD MPRs between endosomes and the TGN in vivo. Stable expression of a dominant negative form of rab9 (S21N) blocked this transport step specifically, while the rates of biosynthetic protein transport and fluid phase and receptor-mediated endocytosis remained unchanged. Moreover, expression of rab9 S21N at only twofold higher levels than wild type rab9 protein was sufficient to yield this phenotype. Although we only monitored the TGN recycling of the 300-kD MPR, it is likely that expression of rab9 S21N also inhibited the recycling of the 45-kD MPR. These results confirm our previous finding that pure rab9 protein had the capacity to stimulate the recycling of 300-kD MPRs to the TGN in an in vitro system that reconstitutes this transport step (Lombardi et al., 1993).

Inhibition of MPR recycling to the TGN had a severe impact on the ability of cells to sort newly synthesized lysosomal enzymes. The delivery of cathepsin D to lysosomes, as monitored by the rate of appearance of the mature form of this protein, was strongly inhibited in N21 cells. In addition, cells expressing rab9 S21N secreted a larger fraction of newly synthesized lysosomal enzymes than control cells.

Cells rendered defective in lysosomal enzyme sorting by expression of rab9 S21N compensated for this defect by increasing their rates of synthesis of a variety of lysosomal enzymes. Endogenous levels of cathepsin D, hexosaminidase and β-glucuronidase were all elevated in N21 cells. A larger fraction of these enzymes were also secreted by the cells, but were at least in part, reinternalized via surface MPRs. In ad-

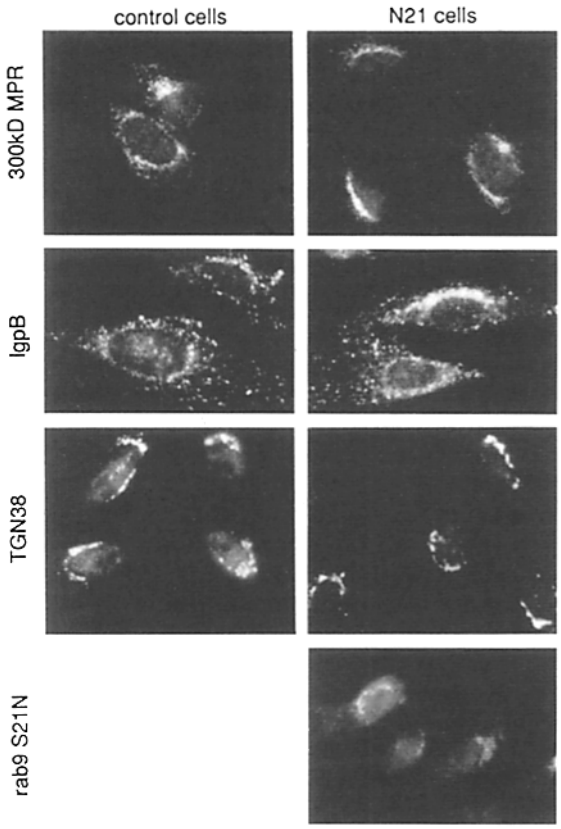

Figure 8. Expression of rab9 S21N has little impact on MPR distribution. Control cells (*left*) or N21 cells (*right*) were grown on collagen-coated coverslips and processed for immunofluorescence microscopy using rabbit anti-300-kD MPR antiserum (1:1,000), mouse anti-lgpB culture supernate, rabbit anti-TGN38 (1:800), or affinity purified rabbit anti-rab9 antibodies (1:100). Slides were viewed using a Zeiss Axiophot microscope fitted with a 100× objective; each row was photographed using identical exposure times. Endogenous rab9 is barely detected by immunofluorescence in control CHO cells due to its very low expression level.

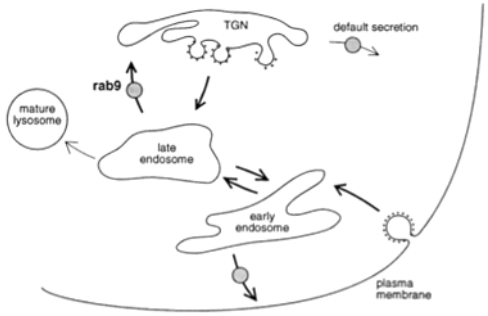

Figure 9. Trafficking pathways taken by mannose 6-phosphate receptors and/or lysosomal enzymes. Bold arrows demarcate MPR pathways; thin arrows represent paths taken by lysosomal enzymes released from MPRs or secreted by default. Rab9 S21N blocked only MPR recycling from late endosomes to the TGN; other pathways appeared to function at normal rates. The rab9 S21N block led to increased default secretion, but did not alter significantly the overall subcellular distribution of MPRs at steady state.

dition to inducing the synthesis of soluble lysosomal enzymes, the level of the lysosomal membrane glycoprotein, lgpB was increased 3.6-fold and MPRs levels increased 1.6-fold. Thus, cells seem to have the capacity to induce the coordinate synthesis of a group of organelle-specific proteins. This is not without precedent; indeed, upon heat shock, a series of ER-localized chaperones are induced (Gething and Sambrook, 1992), and upon compactin treatment, an entire crystalloid smooth ER is induced (Chin et al., 1982).

These experiments confirm that MPRs are limiting in the secretory pathway of N21 cells. While this may be due, in part, to an increase in lysosomal enzyme synthesis, the block in MPR recycling in N21 cells would certainly exacerbate a deficiency in unoccupied, TGN-localized MPRs. The compensatory induction of lysosomal enzymes in N21 cells supports the notion that recycling from the TGN is necessary to maintain an adequate supply of MPRs within the Golgi to accomplish efficient lysosomal enzyme targeting.

MPRs cycle between the TGN and late endosomes in what is referred to as the biosynthetic pathway, and between the cell surface and early endosomes, along the conventional endocytic pathway (Fig. 9). These pathways are interconnected, in that the entire pool of MPRs cycles through the cell surface in less than an hour (Sahagian, 1984; Gartung, 1985). However, it has not yet been established precisely how these pathways are connected. MPRs in the TGN might escape the biosynthetic pathway and be delivered to the surface by default. Alternatively, MPRs might shuttle directly from late endosomes to the cell surface, or from late endosomes to early endosomes, from which they could then recycle to the cell surface. Since a severe block in their transport back to the TGN did not alter their overall cycling properties or their steady state morphological distribution, our data provide the first indication that MPRs can be transported from late endosomes back to the cell surface, either directly, or via early endosomes. Such a pathway has also been documented for a lysosomal membrane glycoprotein in chick fibroblasts (cf., Lippincott-Schwartz and Fambrough, 1986).

Inhibition of MPR recycling to the TGN did not lead to the accumulation of MPRs within a transport-incompetent membrane compartment. Despite a severe decrease in transport to the TGN, MPRs were free to cycle between endosomes and the cell surface. Thus, even though rabs are thought to act in the process of vesicle targeting and/or fusion, the mutant protein did not lead to accumulation of MPRs in non-functional transport vesicles. Rather, MPRs seemed to retain access to other transport pathways. These findings would be consistent with a model in which rab proteins in their GTP conformation are recruited onto nascent transport vesicles. In the absence of GTP rabs, formation of transport vesicles might be inhibited, and/or cargo recruitment might be much less efficient. Further experiments will be needed to explore these possibilities.

We have recently shown that the recruitment of rab9 onto late endosome-enriched membranes is accompanied by nucleotide exchange (Soldati et al., 1994). Prenylated rab9, in its GDP conformation, is delivered to late endosome membranes as a complex with GDI by a process that is saturable both in terms of its overall rate and extent (Soldati et al., 1993, 1994). Rab9 recruitment requires proteins on

the surface of late endosomes, and is inhibited by GDP or excess unoccupied GDI.

Rab9 S21N binds GDP in strong preference to GTP. Despite its expected occurrence in a GDP conformation, a fraction of the protein was prenylated and became membrane associated. Moreover, the protein did not display a random distribution in terms of its membrane association—much like the wild type protein, rab9 S21N colocalized to a large extent with MPRs on late endosomes. Since the equivalent mutation in rab3A generated a protein with enhanced affinity for a nucleotide exchanger, it is possible that the membrane association of rab9 S21N reflects a non-productive interaction with a membrane-associated, rab9 nucleotide exchanger. A yeast protein capable of stimulating the nucleotide exchange of Sec4 has been identified (Moya et al., 1993), and it has been shown to occur in tight association with membranes. If this model for rab9 S21N localization is correct, the properties of rab9 S21N association with membranes would be predicted to differ from those of the wild type protein. It will be of interest to determine if membrane-associated rab9 S21N is in a GDP- or GTP-bound conformation in terms of our understanding of the mechanism of rab protein recruitment. The availability of an in vitro system that reconstitutes selective rab9 membrane association (Soldati et al., 1994) should permit us to investigate this further.

In summary, we have shown that MPR recycling is an important step in the process by which newly synthesized lysosomal enzymes are delivered to lysosomes. Moreover, mutation of a single Ras-like GTPase, rab9, disrupted this process selectively. These findings support the current view that Ras-like GTPases are key regulators of independent intracellular transport steps. The ability of cells to compensate for a block in lysosomal enzyme targeting by a secretion-recapture mechanism underscores the adaptability of eukaryotic cells in terms of their capacity to use salvage pathways to generate and maintain essential organelles.

We are grateful to Dr. Stuart Kornfeld for his generous gift of β-glucuronidase, Drs. W. Sly, I. Mellman and G. Banting for gifts of antibodies, and I. Riederer, M. Copass and C. Peter for expert technical assistance.

This research was funded by grants from the National Institutes of Health (DK37332) and the March of Dimes Birth Defects Foundation. M. A. Riederer and T. Soldati were recipients of postdoctoral fellowships from the Swiss National Research Foundation; A. D. Shapiro was supported by a predoctoral fellowship from the National Science Foundation.

Received for publication 22 November 1993 and in revised form 18 February 1994.

References

Bradford, M. M. 1976. A rapid and sensitive method for the quantitation of microgram quantities of protein utilizing the principle of protein-dye binding. *Anal. Biochem.* 72:248–254.

Bucci, C., R. G. Parton, I. H. Mather, H. Stunnenberg, K. Simons, B. Hoflack, and M. Zerial. 1992. The small GTPase rab5 functions as a regulatory factor in the endocytic pathway. *Cell.* 70:715–728.

Burnette, W. N. 1981. "Western blotting": electrophoretic transfer of proteins from SDS-polyacrylamide gels to unmodified nitrocellulose and radiographic detection with antibody and radiolabeled protein A. *Anal. Biochem.* 112:195–203.

Burstein, E. S., W. H. Brondyk, and I. G. Macara. 1992. Amino acid residues in the Ras-like GTPase rab3A that specify sensitivity to factors that regulate the GTP/GDP cycling of rab3A. *J. Biol. Chem.* 267:22715–22718.

Chege, N. W., and S. R. Pfeffer. 1990. Compartmentation of the Golgi complex: brefeldin-A distinguishes trans Golgi cisternae from the trans Golgi network. *J. Cell Biol.* 111:893–899.

Chin, D. J., K. L. Luskey, R. G. Anderson, J. R. Faust, J. L. Goldstein, and M. S. Brown. 1982. Appearance of crystalloid endoplasmic reticulum in compactin-resistant Chinese hamster cells with a 500-fold increase in 3-hydroxy-3-methylglutaryl-coenzyme A reductase. *Proc. Natl. Acad. Sci. USA.* 79:1185–1189.

Duncan, J., and S. Kornfeld. 1988. Intracellular movement of two mannose 6-phosphate receptors: return to the Golgi apparatus. *J. Cell Biol.* 106: 617–628.

Erickson, A. H., and G. Blobel. 1983. Carboxyl-terminal proteolytic processing during biosynthesis of the lysosomal enzymes beta-glucuronidase and cathepsin D. *Biochemistry.* 22:5201–5205.

Farnsworth, C. L., and L. A. Feig. 1991. Dominant inhibitory mutations in the Mg^{++}-binding site of RasH prevent its activation by GTP. *Mol. Cell. Biol.* 11:4822–4829.

Feig, L. A., and G. M. Cooper. 1988. Inhibition of NIH 3T3 cell proliferation by mutated Ras proteins with preferential affinity for GDP. *Mol. Cell. Biol.* 8:3235–3243.

Gartung, C., T. Braulke, A. Hasilik, and K. von Figura. 1985. Internalization of blocking antibodies against mannose-6-phosphate specific receptors. *EMBO (Eur. Mol. Biol. Organ.) J.* 4:1725–1730.

Gething, M. J., and J. Sambrook. 1992. Protein folding in the cell. *Nature (Lond.).* 355:33–45.

Geuze, H. J., J. W. Slot, G. J. Strous, A. Hasilik, and K. von Figura. 1984. Ultrastructural localization of the mannose 6-phosphate receptor in rat liver. *J. Cell Biol.* 98:2047–2054.

Geuze, H. J., J. W. Slot, G. J. Strous, A. Hasilik, and K. von Figura. 1985. Possible pathways for lysosomal enzyme delivery. *J. Cell Biol.* 101: 2253–2262.

Geuze, H. J., W. Stoorvogel, G. J. Strous, J. W. Slot, J. E. Bleekemolen, and I. Mellman. 1988. Sorting of mannose 6-phosphate receptors and lysosomal membrane proteins in endocytic vesicles. *J. Cell Biol.* 107:2491–2501.

Goda, Y., and S. R. Pfeffer. 1988. Selective recycling of the mannose 6-phosphate/IGF-II receptor to the trans Golgi network in vitro. *Cell.* 55:309–320.

Gorvel, J. P., P. Chavrier, M. Zerial, and J. Gruenberg. 1991. rab5 controls early endosome fusion in vitro. *Cell.* 64:915–925.

Griffiths, G., B. Hoflack, K. Simons, I. Mellman, and S. Kornfeld. 1988. The mannose 6-phosphate receptor and the biogenesis of lysosomes. *Cell.* 52:329–341.

Griffiths, G., R. Matteoni, R. Back, and B. Hoflack. 1990. Characterization of the cation-independent mannose 6-phosphate receptor-enriched prelysosomal compartment in NRK cells. *J. Cell Sci.* 95:441–461.

John, J., H. Rensland, I., Schlichting, I. Vetter, G. D. Borasio, R. S. Goody, and A. Wittinghofer. 1993. Kinetic and structural analysis of the Mg^{2+}-binding site of the guanine nucleotide-binding protein $p21^{H\text{-}ras}$. *J. Biol. Chem.* 268:923–929.

Kingsley, D. M., K. F. Kozarsky, L. Hobbie, and M. Krieger. 1986. Reversible defects in O-linked glycosylation and LDL receptor expression in a UDP-Gal/UDP-GalNAc 4-epimerase deficient mutant. *Cell.* 44:749–759.

Kornfeld, S. 1992. Structure and function of the mannose 6-phosphate/insulin-like growth factor receptors. *Annu. Rev. Biochem.* 61:307–330.

Kornfeld, S., and I. Mellman. 1989. The biogenesis of lysosomes. *Annu. Rev. Cell Biol.* 5:483–525.

Laemmli, U. K. 1970. Cleavage of structural proteins during assembly of the head of bacteriophage T4. *Nature (Lond.).* 227:680–685.

Lippincott-Schwartz, J., and D. M. Fambrough. 1986. Lysosomal membrane dynamics: structure and interorganellar movement of a major lysosomal membrane glycoprotein. *J. Cell Biol.* 102:1593–1605.

Lombardi, D., T. Soldati, M. A. Riederer, Y. Goda, M. Zerial, and S. R. Pfeffer. 1993. Rab9 functions in transport between late endosomes and the trans Golgi network. *EMBO (Eur. Mol. Biol. Organ.) J.* 12:677–682.

Maniatis, T., E. Fritsch, and J. Sambrook. 1989. Molecular Cloning Laboratory Manual. Cold Spring Harbor Laboratory, Cold Spring Harbor, NY.

Marsh, M., S. Schmid, H. Kern, E. Harms, P. Male, I. Mellman, and A. Helenius. 1987. Rapid analytical and preparative isolation of functional endosomes by free flow electrophoresis. *J. Cell Biol.* 104:875–886.

Miettinen, H. M., J. K. Rose, and I. Mellman. 1989. Fc receptor isoforms exhibit distinct abilities for coated pit localization as a result of cytoplasmic domain heterogeneity. *Cell.* 58:317–327.

Moya, M., D. Roberts, and P. Novick. 1993. DSS4-1 is a dominant suppressor of Sec4-8 that encodes a nucleotide exchange protein that aids Sec4p function. *Nature (Lond.).* 361:460–463.

Novick, P., C. Field, and R. Schekman. 1980. Identification of 23 complementation groups required for post-translational events in the yeast secretory pathway. *Cell.* 21:205–215.

Pai, E. F., W. Kabsch, U. Krengel, K. C. Holmes, J. John, and A. Wittinghofer. 1989. Structure of the guanine-nucleotide binding domain of the Ha-ras oncogene product p21 in the triphosphate conformation. *Nature (Lond.).* 341:209–214.

Pai, E. F., U. Krengel, G. A. Petsko, R. S. Goody, W. Kabsch, and A. Wittinghofer. 1990. Refined crystal structure of the triphosphate conformation of Ha-ras at 1.35 Å resolution: implications for the mechanism of GTP hydrolysis. *EMBO (Eur. Mol. Biol. Organ.) J.* 9:2351–2359.

Pfeffer, S. R. 1987. The endosomal concentration of a mannose 6-phosphate receptor is unchanged in the absence of ligand synthesis. *J. Cell Biol.* 105:229–234.

Pfeffer, S. R. 1992. GTP-binding proteins in intracellular transport. *Trends Cell*

Biol. 2:41–46.

Plutner, H., A. D. Cox, S. Pind, R. Khosravi-Far, J. R. Bourne, R. Schwaninger, C. J. Der, and W. E. Balch. 1991. Rab1b regulates vesicular transport between the endoplasmic reticulum and successive Golgi compartments. *J. Cell Biol.* 115:31–43.

Rexach, M., and R. Schekman. 1991. Distinct Biochemical Requirements for the Budding, Targeting and Fusion of ER-derived Transport Vesicles. *J. Cell Biol.* 114:219–229.

Robbins, A. R. 1979. Isolation of lysosomal α-mannosidase mutants of Chinese hamster ovary cells. *Proc. Natl. Acad. Sci. USA.* 76:1911–1915.

Rosenfeld, M. G., G. Kreibich, D. Popov, K. Kato, and D. D. Sabatini. 1982. Biosynthesis of lysosomal hydrolases: their synthesis on bound polysomes and the role of co- and post-translational processing in determining their subcellular distribution. *J. Cell Biol.* 93:135–143.

Sahagian, G. G. 1984. The mannose 6-phosphate receptor: function, biosynthesis and translocation. *Biol. Cell.* 51:207–214.

Sahagian, G. G., and E. F. Neufeld. 1983. Biosynthesis and turnover of the mannose 6-phosphate receptor in cultured Chinese Hamster Ovary cells. *J. Biol. Chem.* 258:7121–7128.

Segev, N. 1991. Mediation of the attachment or fusion step in vesicular transport by the GTP-binding Ypt1 protein. *Science (Wash. DC).* 252: 1553–1556.

Shapiro, A. D., M. A. Riederer, and S. R. Pfeffer. 1993. Biochemical analysis of rab9, a *ras*-like GTPase involved in protein transport from late endosomes to the *trans* Golgi network. *J. Biol. Chem.* 268:6925–6931.

Soldati, T., M. A. Riederer, and S. R. Pfeffer. 1993*a*. Rab GDI: a solubilizing and recycling factor for rab9 protein. *Mol. Biol. Cell.* 4:425–434.

Soldati, T., A. D. Shapiro, A. B. Dirac-Svejstrup, and S. R. Pfeffer. 1994. Nucleotide exchange accompanies membrane targeting of rab9 protein. *Nature (Lond.).* In press.

Studier, F. A., Rosenberg, J. Dunn, and J. Dubendorff. 1990. Use of T7 RNA polymerase to direct expression of clonal genes. *Methods Enzymol.* 185: 60–86.

Sunyer, T., J. Codina, and L. Birnbaumer. 1984. GTP hydrolysis by pure N_i, the inhibitory regulatory component of adenyl cyclases. *J. Biol. Chem.* 259:15447–15451.

Tisdale, E. J., J. R. Bourne, R. Khosravi-Far, C. J. Der, and W. E. Balch. 1992. GTP binding mutants of rab1 and rab2 are potent inhibitors of vesicular transport from the ER to the Golgi complex. *J. Cell Biol.* 119:749–761.

van der Sluijs, P., M. Hull, P. Webster, P. Mâle, B. Goud, and I. Mellman. 1992. The small GTP binding protein rab4 controls an early sorting event in the endocytic pathway. *Cell.* 70:729–740.

Warren, G., J. Davoust, and A. Cockcroft. 1984. Recycling of transferrin receptors in A431 cells is inhibited during mitosis. *EMBO (Eur. Mol. Biol. Organ.) J.* 3:2217–2225.

Zerial, M., and H. Stenmark. 1993. Rab GTPases in vesicular transport. *Curr. Opin. Cell Biol.* 5:613–619.